Seismic Fragility Analysis of a KSNP Containment Building for Near Fault Earthquakes

In-Kil Choi[1], Young-Sun Choun[1], Seong-Moon Ahn[1], Jeong-Moon Seo[1]
1) Integrated Safety Assessment Division, Korea Atomic Energy Research Institute, Daejeon, Korea

Abstract

In general, near-fault ground motion records exhibit a distinctive long period pulse like a time history with very high peak velocities. It can be expected that a reinforced concrete containment would show a highly nonlinear behavior for a strong near fault ground motion. In this study, the seismic fragility of KSNP (Korean Standard Nuclear Power Plant) containment buildings was estimated by performing a nonlinear seismic analysis for near fault earthquakes. A lumped mass model of the containment building was used for a nonlinear dynamic time history analysis. A tri-linear skeleton curve was used for the nonlinear behavior of the prestressed concrete containment building. In order to estimate the inelastic nonlinear response of containment, the maximum point oriented model was used for the hysteretic rule of a shear deformation. The seismic fragility of a containment building was estimated for several failure criteria, stress and displacement based criteria.

INTRODUCTION

The seismic safety of a nuclear power plant can not be secured by considering only a design basis earthquake as more knowledge on a seismological situation of a nuclear power plant site is gained through the advances in geosciences. In Korea, a survey on some of the Quaternary fault segments near Korean nuclear power plants is ongoing [1]. Some Quaternary fault systems being surveyed are located near a nuclear power plant sites in Korea. It is likely that these faults will be identified as active ones. If the faults are confirmed as active ones, it will be necessary to reevaluate the seismic safety of the nuclear power plants located near these faults. Considering this site condition, near-fault earthquakes can occur at a nuclear power plant site near these potential active faults.

Near-fault ground motions are the ground motions that occur near an earthquake fault. In general, near-fault ground motion records exhibit a distinctive long period pulse like a time history with very high peak velocities. These features are induced by the slip of an earthquake fault. Near-fault ground motions, which have caused much of the damage in recent major earthquakes, can be characterized by a pulse-like motion that exposes a structure to a high input energy at the beginning of a motion. These near-fault ground motions can cause severe damage to the concrete structures in a nuclear power plant due to a high energy input and a distinct nonlinear behavior of concrete structures.

In this study, a KSNP containment structure was selected for an evaluation of the near-fault ground motion effects on concrete structures. The seismic fragility analysis was performed to evaluate the seismic safety of a containment building for near-fault earthquakes based on the nonlinear dynamic time-history analyses.

MODELING OF THE KSNP CONTAINMENT BUILDING

The containment building is a very important structure in a nuclear power plant. It is a final barrier to protect the release of radioactive material to the environment. In Korea, several types of containment buildings have been constructed. The first one is a prestressed concrete containment building which is a typical containment structure for a KSNP. Most of the NPPs in Korea are KSNP. The second one is a prestressed concrete containment building which is a typical containment structure for a CANDU NPP. But the shape and dynamic characteristics are very similar from the point of view of their seismic response. So, a KSNP containment was selected for this study.

Characteristics of KSNP containment building

The KSNP containment building consists of a cylindrical post-tensioned shell having a hemispherical dome. Fig. 1 shows the KSNP containment building. The containment building is structurally independent of other buildings. The cylindrical portion and the hemispherical dome of the structure are prestressed by a post-tensioning system consisting of horizontal and vertical tendons. Three buttresses are equally spaced around the perimeter of the containment building. The inside face of the containment building is steel lined with 1/4-inch plate to ensure a high degree of leak tightness.

Analysis model

Three dimensional finite element models were used for the eigenvalue analysis of the containment buildings. Fig. 2 (a) and (b) show the three-dimensional finite element model and its fundamental mode shape, respectively. All of the containment buildings in Korea are constructed on a competent rock. The soil-structure interaction effect on the dynamic behavior of the containment building is negligible. It was assumed that the containment was fixed to the foundation. The eigenvalue analysis by using the three-dimensional FE model was performed to verify the dynamic characteristics of a lumped mass model that was developed for the efficient nonlinear seismic analysis.

Fig. 2 (c) shows a lumped mass model that was used for the seismic design of the containment building in the design stage. The fundamental frequencies obtained from the finite element models and the lumped mass models are summarized in Table 1 with the fundamental frequencies described in the design reports [2]. As shown in this table, the fundament frequencies of the containment building by the 3-D FE model and the lumped mass model were 4.48 Hz and 4.56 Hz, respectively. This result shows that the fundament frequencies from the lumped mass models coincided well with those from the 3-D FE models and the design reports. The higher modes also show a good agreement. So it can be concluded that the lumped mass model can be used to approximate the 3-D FE model for a nonlinear dynamic time history analysis.

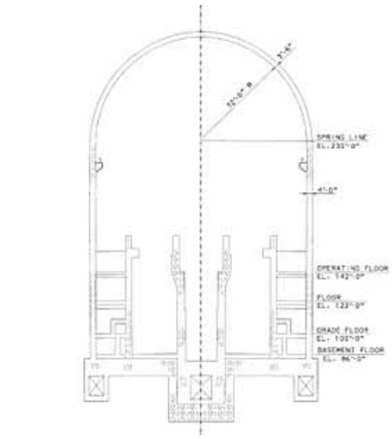

Fig. 1 KSNP containment building

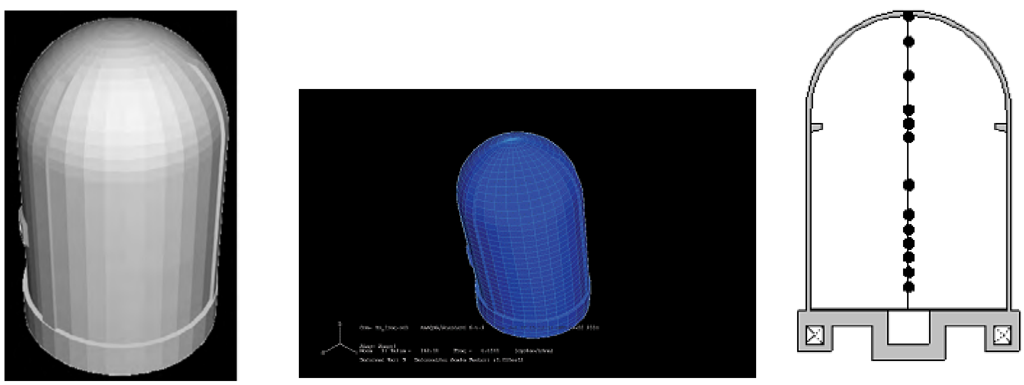

(a) 3-D FEM model (b) Fundamental mode shape (c) Lumped Mass Model

Fig. 2 3-D FE Model, Fundamental Mode Shape and Lumped Mass Model of the Containment Building

Table 1. Fundamental Frequencies of the Containment Building

	3-D FE Model	Lumped Mass Model	Design Report
Frequency(Hz)	4.48	4.56	4.56*

SEISMIC ANALYSIS OF CONTAINMENT BUILDING

Input Ground Motions

The input ground motions for the seismic response analysis to estimate the median response at a certain PGA (Peak Ground Acceleration) level were 10 sets of near-fault ground motion records which had occurred throughout the world. The near-fault earthquake records used for the seismic analysis are listed in Table 2. This earthquake records were obtained from the PEER strong motion data base [3]. Fig. 3 shows the response spectra of the near-fault ground motions normalized to 1.0g PGA. The KSNP containment building was designed by using the standard response spectrum proposed by U.S. NRC Regulatory 1.60 [4] as a design earthquake. The artificial acceleration time histories that envelop the design spectrum were generated by using the CARES program [5]. Fig. 4(a) shows the response spectra of the 20 generated artificial acceleration time histories. Fig. 4(b) shows the mean response spectrum of the generated time histories with the target response spectrum. Fig. 4 (c) shows one of the generated acceleration time histories anchored to 0.1g PGA.

Table 2. List of the Near-Fault Ground Motions

Earthquake	Date	Station Name	Closest to Fault Rupture(km)	Closest to Surface Projection of Rupture(km)	Magnitude	PGA(g)	PGV (cm/sec)
Imperial Valley	1979-10-15	952 El Centro Array #5	1.00	4.00	6.5	0.379	90.5
Imperial Valley	1979-10-15	942 El Centro Array #6	1.00	1.30	6.5	0.439	109.8
Kocaeli, Turkey	1999-08-17	Arcelik	17.00	17.00	7.4	0.149	39.5
Kocaeli, Turkey	1999-08-17	Yarimca	2.60	2.60	7.4	0.268	65.7
Northridge	1994-01-17	0655 Jensen Filter Plant	6.20	-	6.7	0.424	106.2
Northridge	1994-01-17	74 Sylmar - Converter Sta	6.20	0.20	6.7	0.612	117.4
SuperStition Hills	1987-11-24	5051 Parachute Test Site	0.70	-	6.7	0.455	112.0
Chi-Chi, Taiwan	1999-09-20	TCU052	0.24	0.06	7.6	0.419	118.4
Chi-Chi, Taiwan	1999-09-20	TCU068	1.09	0.50	7.6	0.462	263.1
Chi-Chi, Taiwan	1999-09-20	TCU075	1.49	1.49	7.6	0.333	88.3

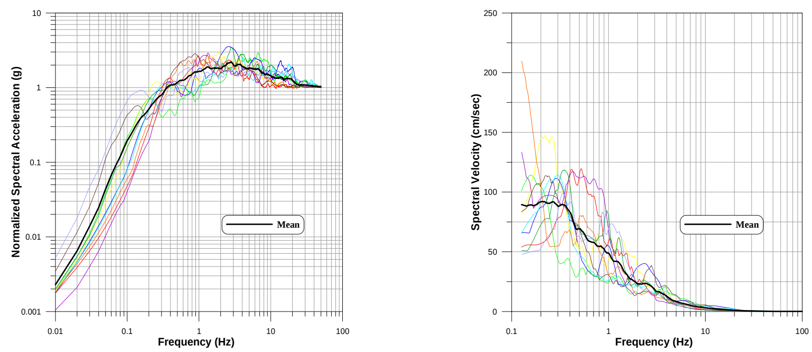

(a) Acceleration (b) Velocity

Fig. 3 Response Spectra of Near-Fault Ground Motions

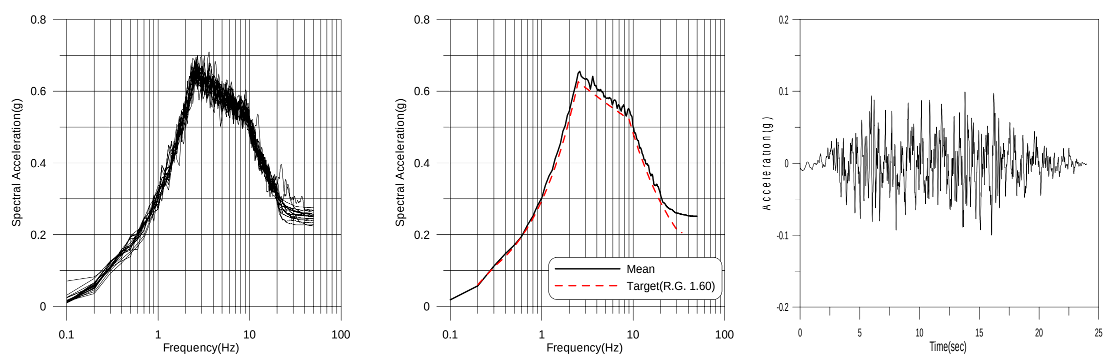

(a) Acceleration Response Spectra (b) Mean Response Spectrum (c) Acceleration Time History

Fig. 4 Acceleration Response Spectra and Time History of Design Earthquake

Nonlinear Seismic Analysis

In this study, the tri-linear approximation shown in Fig. 5 (a) was used for the shear behavior of the containment building. This skeleton curve is of the lower part of the containment shell. The turning points for the shear stress and strain relationship were determined based on the EPJR (Electric Power Joint Research) method [6]. The skeleton curves of each part are very similar, since the containment shell has similar dimension and detail throughout the entire wall height. In order to perform the elasto-plastic seismic response analysis, based on the tri-linear skeleton curve, the maximum point oriented model was used as a hysteresis rule for the repeated unloading and loading processes. Fig. 5 (b) and (c) shows the hysteresis rules, the maximum point oriented model and degraded model, for the shear force-displacement relation and moment-curvature relation, respectively. The time history analysis method was used for the nonlinear seismic response analysis of the containment building. The TDAP IIID program [7] was used for the nonlinear time history analysis.

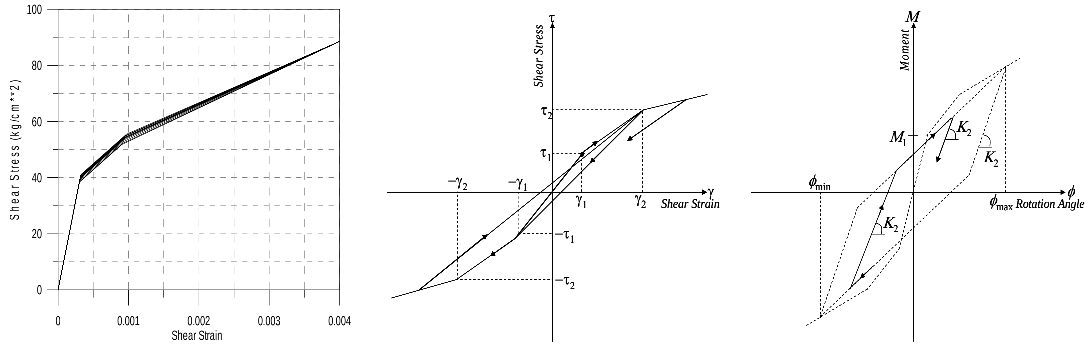

(a) Tri-linear Skeleton Curves for Shear (b) Maximum Point-oriented Model (c) Degraded Model

Fig. 5 Nonlinear Material Model of Containment Shell

Seismic Response of Containment Building

The nonlinear inelastic dynamic analyses were performed to investigate the seismic response of the containment buildings for near-fault earthquakes. In the design stage, the elastic analysis was performed to obtain the member stress and floor acceleration response. The response spectrum analysis method is generally used for the seismic design of a NPP containment building in Korea.

Fig. 6 shows the maximum seismic response of the containment buildings, the maximum top displacement, the maximum base shear and the maximum story drift, according to the peak ground acceleration of the near-fault earthquakes. The solid line represents the mean response. It is shown that the displacement responses are increased more rapidly than the force response. Also the variation of the displacement response according to the input ground motion is larger than that of the force response, especially in the strong ground motion range.

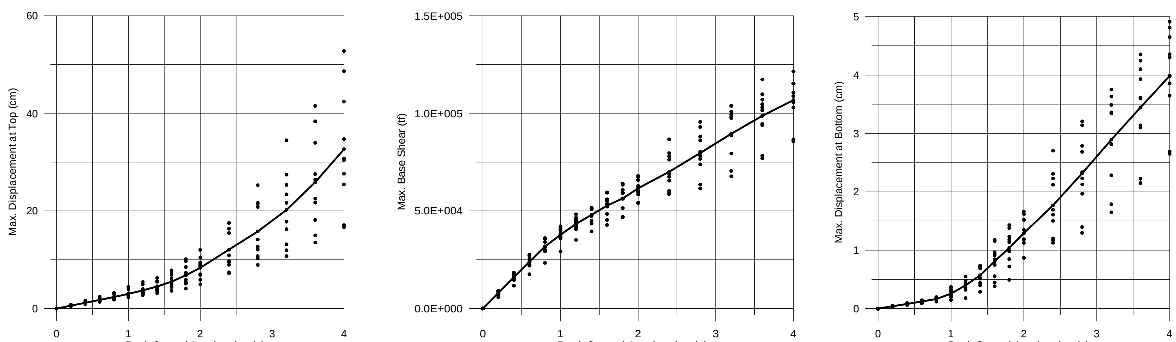

(a) Maximum Top Displacement (b) Maximum Base Shear (c) Maximum Story Drift

Fig. 6 Maximum Response of Containment Building

Fig. 7 shows the shear force–displacement and moment-curvature relationship at 1.0g PGA, respectively. It definitely shows an inelastic nonlinear response. Fig. 7 shows the comparison of the maximum displacement response with that for the design ground motion. The maximum displacement response is rapidly increased from 0.8g PAG for the NRC ground motion due to the nonlinear response.

Fig. 8 shows the normalized maximum mean displacement and shear force ratio for the linear elastic response. It is observed from Fig. 8 (a) that the maximum displacement response is increased rapidly for the design ground motion. The displacement ratio is increased up to 2.3 at 1.8g PGA. The displacement ratio for the near fault ground motion is not so great. Fig. 8 (b) shows the normalized maximum shear force ratio for the linear elastic response. The maximum shear force is considerably reduced in the strong ground motion range. This is due to an increase of the inelastic energy absorption rate caused by a nonlinear response of the containment building. In these figures, it can be easily established whether the containment behaves in a linear elastic range or not at a certain PGA level. The containment shows a nonlinear response from 0.6g PGA for the design ground motion and the near fault ground motions.

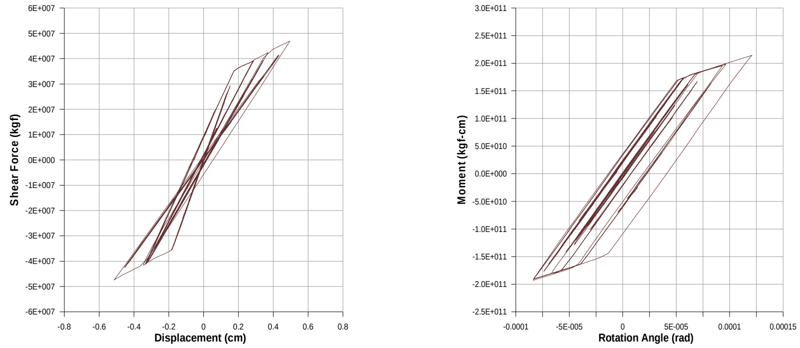

(a) Shear (b) Moment

Fig. 7 Hysteretic Behavior of Containment Building for Strong Ground Motion

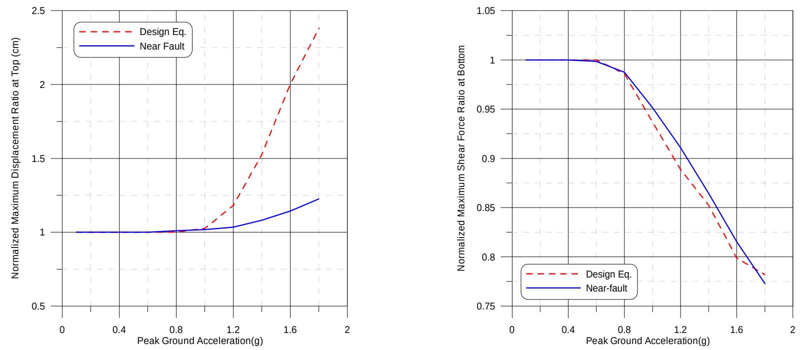

(a) Maximum Displacement at Top (b) Maximum Shear Force at Bottom

Fig. 8 Normalized Response Ratios to the Linear Elastic Response

SEISMIC FRAGILITY ANALYSIS

Fragility Calculation Method

The safety margin of a member of a structure for the present level of seismic a intensity is defined as a ratio of its seismic capacity to its seismic response [8]. Safety margin $S_f(a)$ concerning some seismic response parameters for a given seismic intensity a is defined as the ratio of its seismic capacity R to the seismic response parameter $S(a)$, i.e.

$$S_f(a) = R / S(a) \tag{1}$$

and the probability of a failure is

$$P_f(a) = \mathrm{Prob}(R / S(a) < 1) \tag{2}$$

The seismic fragility of a structure probabilistically represents the capability of a ground motion to cause structural damage. The probability of a failure of a structure $P_f(a)$ at any non-exceedence probability level Q can be obtained from the following equation.

$$P_f(a) = \phi\left(\frac{\ln(S_m(a)/C_m) + \beta_U \phi^{-1}(Q)}{\beta_R}\right) \tag{3}$$

where $\phi(\cdot)$ is the standard Gaussian cumulative distribution function, a is a peak ground acceleration as a ground motion parameter, $\phi^{-1}(\cdot)$ is the inverse of the standard Gaussian cumulative distribution function, $S_m(a)$ and C_m are the median seismic response at a given ground acceleration a, and the median seismic capacity, respectively, and β_R and β_U are the lognormal standard deviations of the randomness and uncertainty of $S_m(a)$ and C_m, respectively.

In this study, the median ground acceleration capacity was calculated from the result of the non-linear seismic response analyses. For a variate a which follows a log-normal distribution, the median response S_m and the log-normal standard deviation of the response β_a at a given acceleration level can be expressed by its mean μ_a and the coefficient of a variation δ_a [9].

$$S_m = \frac{\mu_a}{\sqrt{1+\delta_a^2}} \tag{4}$$

$$\beta_a^2 = \ln\left(1+\delta_a^2\right) \tag{5}$$

Median Response

Regression analysis was performed to estimate the mean response according to the peak ground acceleration level. As shown in Fig. 9, the displacement response can be divided into two parts, linear and non-linear. A regression analysis was performed for an individual part by a linear and polynomial fit. The regression analysis was used to determine the median ground acceleration capacity for the input ground motions. The median response used for the seismic fragility of Eq. (3) can be obtained from the mean response by Eq. (4)

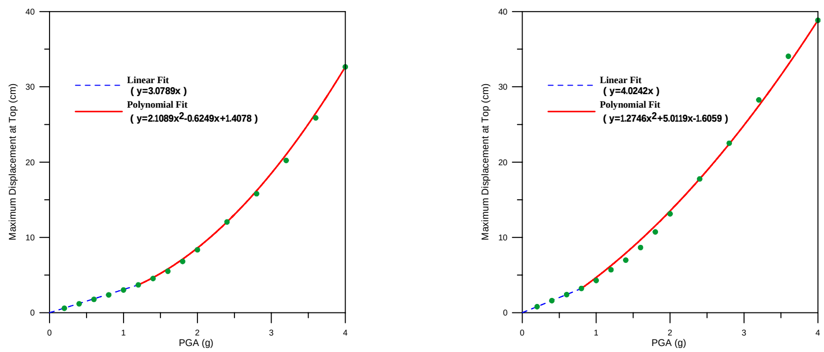

(a) For Near-Fault (b) For Design Earthquake

Fig. 9 Regression of the Mean Top Displacement

Failure Mode and Criteria

In a fragility analysis, it is very important to estimate various failure modes and failure criteria. In general, the shear failure at a lower part of the containment shell was used as a dominant failure mode. The ultimate shear stress and bending moment capacity at a lower part of the containment shell were generally used as the dominant failure criteria of the containment building. This conventional method was based on a linear elastic seismic analysis. The effect of the non-linear behavior of a structure is considered by using the inelastic energy absorbing factor [8]. In this study, the non-linear seismic time history analyses for the near-fault ground motions were performed to estimate the non-linear behavior of the containment building for the strong ground motions.

In this study, three kinds of damage index were used. The top displacement and story drift are used as the damage indexes of the containment building. Accordingly, with the current state-of-the-art technology, it is believed to be sufficient to define the limit states for a reliability analysis purpose in terms of the overall inelastic deformation or maximum inter-story drift of a structural system [10]. The top displacement is very useful for the damage index of a containment building, since a containment building is usually a very simple cantilever type structure. To obtain the failure criteria for the fragility analysis, a pushover analysis was performed. Fig. 10 shows the pushover analysis model and the results for the containment building.

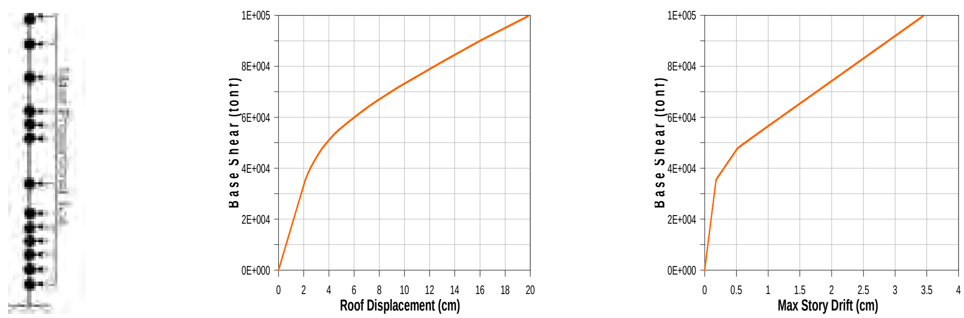

(a) Pushover analysis model (b) Top Displacement (c) Story Drift

Fig. 10 Pushover Analysis Model and Results

Two damage indices were used for the failure criteria. The first one is the occurrence of a crack in the containment shell. The crack will occur in the containment shell at the yielding of the concrete. The second one is a collapse of the containment building. The collapse of the containment building was defined as when the containment shell reaches its ultimate displacement

The logarithmic standard deviations for a randomness and uncertainty are shown in Table 2. The logarithmic standard deviation for a randomness is determined by Eq. (5). In this study, a variation of the response is assumed to be caused by the randomness of the earthquake ground motions. It was assumed that an uncertainty is caused by a variation of the structural capacity. The logarithmic standard deviation for an uncertainty was obtained from reference [11].

Table 2. Logarithmic Standard Deviation for Randomness and Uncertainty

Failure Criteria		Near-Fault	Design Earthquake
Base Shear	Randomness(β_R)	0.117	0.049
	Uncertainty(β_U)	0.211	0.211
Top Displacement	Randomness(β_R)	0.274	0.113
	Uncertainty(β_U)	0.211	0.211
Story Drift	Randomness(β_R)	0.230	0.107
	Uncertainty(β_U)	0.211	0.211

The realistic seismic capacity of the structures and equipments in a SPRA (Probabilistic Seismic Risk Assessment) can be expressed by the fragility curves or HCLPF (High Confidence Low Probability of Failure) capacity. HCLPF capacity in a SPRA is defined mathematically as a 95% confidence of less than a 5% probability of failure. This HCLPF capacity is generally used as an index to represent the seismic capacity of structures and equipments in the seismic safety evaluation. The HCLPF capacity may be computed from the following equation. Table 3 shows the median and HCLPF capacity of the containment building.

$$HCLPF = A_m \cdot \exp[-1.65(\beta_R + \beta_U)] \tag{6}$$

Table 3. Median and HCLPF Capacity of Containment

Failure Criteria		Crack		Failure	
		HCLPF(g)	Median(g)	HCLPF(g)	Median(g)
Base Shear	Near-Fault	0.52	0.94	1.52	3.06
	Design Eq.	0.46	0.77	1.42	2.68
Top Displ.	Near-Fault	0.27	0.73	1.55	2.72
	Design Eq.	0.26	0.53	1.39	2.19
Story Drift	Near-Fault	0.36	0.83	1.86	3.16
	Design Eq.	0.35	0.66	1.65	2.65

Fig. 11 shows the fragility curves of the containment building for the near-fault ground motions and design earthquake. The fragility for a design earthquake shows a higher fragility than that for the near-fault ground motions. It means that the design earthquake has enough margins for the near-fault ground motions which can occur near from the NPP sites.

Fig. 12 shows a comparison of the mean fragility curves according to the failure criteria. The seismic fragility based on the ultimate displacement shows a higher probability of failure than those based on the other failure criteria. It can be known from these figures that the stress based failure criteria is not conservative and can not consider properly the nonlinear hysteretic behavior of a concrete containment building at a strong ground motion level. It is necessary to consider a nonlinear behavior for a seismic fragility of a concrete structure which shows a highly nonlinear behavior.

CONCLUSION

In this study, the seismic fragility analysis of a KSNP containment building was performed based on the responses obtained from the inelastic nonlinear seismic analyses for near-field ground motions.

The displacement responses due to the near-field ground motions were smaller than those due to the design ground motion. The near-fault ground motion which has a long period pulse like a time history with very high peak velocities did not significantly affect the safety of the containment building, since it is a relatively stiff structure and has a higher fundamental frequency than the dominant frequency of the near-fault ground motions. This result shows that the near-fault ground motion effects are not so damaging to a nuclear power plant structure which is a relatively stiff structure, such as a containment building.

In the seismic fragility analysis for the probabilistic seismic safety assessment, the seismic safety of the NPP structures was estimated based on a stress response. It is not enough to estimate the seismic safety of a structure by a stress response. A displacement response is a very important factor for the seismic safety of a structure. A displacement based seismic fragility analysis is essential to estimate the seismic margin of the containment building when considering a nonlinear dynamic behavior. A displacement based seismic fragility analysis method is suitable for considering the non-linear hysteretic seismic behavior of a concrete containment building.

For an exact evaluation of the seismic fragility of a concrete structure, it is necessary to evaluate the ultimate displacement capacity and its variation based on seismic tests and analyses results.

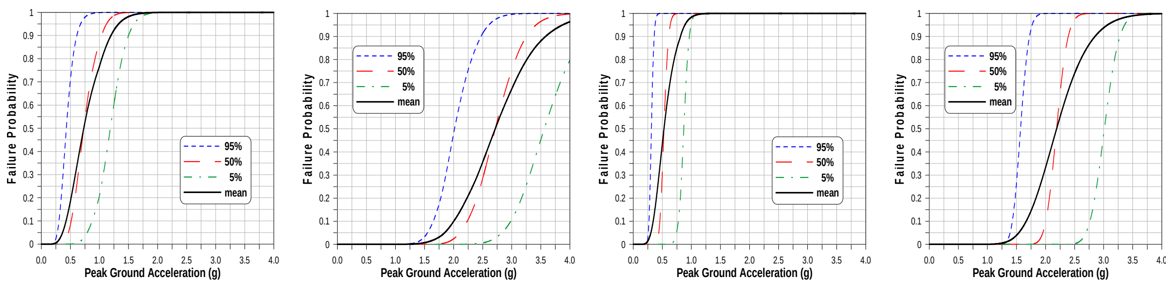

(a) Crack for Near-Fault (b) Collapse for Near-Fault (c) Crack for Design (d) Collapse for Design

Fig. 11 Fragility Curves of the Containment Building

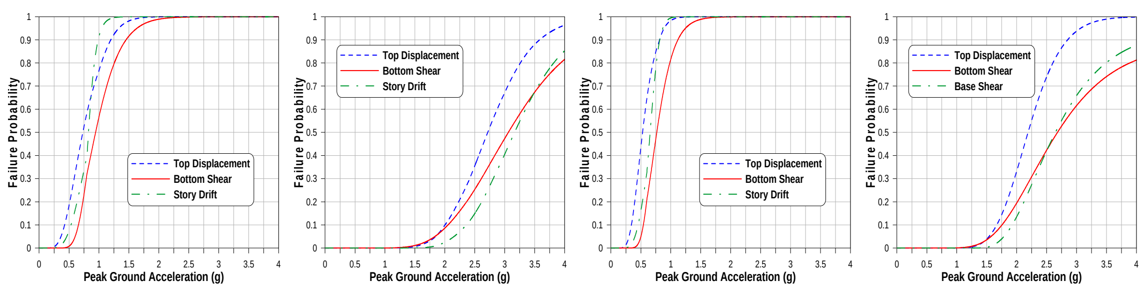

(a) Crack for Near-Fault (b) Collapse for Near-Fault (c) Crack for Design (d) Collapse for Design

Fig. 12 Comparison of the Mean Fragility Curve According to the Failure Criteria

ACKNOWLEDGEMENT

This research was supported by the Mid- and Long-Term Nuclear Research & Development Program of the Ministry of Science and Technology, Korea.

REFERENCES

1. Korea Institute of Nuclear Safety, *Development of Seismic Safety Evaluation Technology for NPP Sites*, KINS/GR-206, 2000.
2. Korea Power Engineering Company, Inc. and Sargent & Lundy, *Design Report : Containment Shell and Dome*, Report No. 9-310-C409-003, Rev. 0, July 16, 1990.
3. PEER Strong Motion Database, http://peer.berkeley.edu/nga/.
4. NRC, US NRC Regulatory Guide 1.60, *Design Response Spectra for Seismic Design of Nuclear Power Plants*, 1973.
5. Brookhaven National Laboratory, *CARES (Computer Analysis for Rapid Evaluation of Structures)*, Ver. 1.0, NUREG/CR-5588, Vol. 2, 1990..
6. Park, Y. J. and C. H. Hofmayer, *Technical Guidelines for Aseismic Design of Nuclear Power Plants*, Translation of JEAG 4601-1987, NUREG/CR-6241, 1994.
7. ARK Information System, *TDAPⅢ*, Ver 2.13, 2005.
8. R. P. Kennedy and M. K. Ravindra, "Seismic Fragilities for Nuclear Power Plant Risk Studies," *Nuclear Engineering and Design*, 79, 1984.
9. Ang ZH-s, Tang W. H., *Probability Concepts in Engineering Planning and Design, Basic Principles*, Vol. 1, Wiley, New York, 1975.
10. Bruce R. Ellingwood, "Earthquake Risk Assessment of Building Structures", *Reliability Engineering and System Safety*, 74, 2001.
11. M. Ozaki, A. Okazaki, K. Tomomoto, T. Iba, R. Satoh, H. Nanba, H. Seya, K. Moriyama, and T. Ugata, "Improved Response Factor Methods for Seismic Fragility of Reactor Building," *Nuclear Engineering and Design*, 185, 1998.